DOI: 10.1002/cbic.200800158

Blue-Light Induced Interaction of LOV Domains from *Chlamydomonas reinhardtii*

Roger J. Kutta,[a] Edith S. A. Hofinger,[b] Hendrik Preuss,[b] Günther Bernhardt,*[b] and Bernhard Dick*[a]

The phototropin from Chlamydomonas reinhardtii *is a 120 kDa blue light receptor that plays a key role in gametogenesis of this green alga. It comprises two light-sensing domains termed LOV1 and LOV2 (**l**ight **o**xygen and **v**oltage) and a serine/threonine kinase domain. The post-translationally incorporated chromophore is flavin mononucleotide (FMN). Upon absorption of blue light, LOV domains undergo a photocycle that activates a Ser/Thr kinase. The mechanism of this activation is still unknown. We studied the oligomerization of the recombinant LOV1 domain (amino acids 16–133) of* C. reinhardtii *by means of UV/Vis spectroscopy, size-exclusion chromatography (SEC), and chemical cross-linking with glutardialdehyde. The thermal back-reaction of LOV1 from the signaling state to the dark state as monitored by UV/Vis spectroscopy after an intensive blue light pulse could not be explained by a monoexponential model, although the spectra did not indicate the presence of an additional species. Therefore, we investigated the quaternary structure of the LOV1 domain by size-exclusion chromatography in the dark. This revealed an equilibrium between dimers and higher oligomers ($M_W > 200$ kDa) under native conditions. No monomers were detected by SEC. However, by analysis of the equilibrium by cross-linking of the protein with glutardialdehyde and subsequent SDS-PAGE, monomers and dimers were identified. Exposure of LOV1 to blue light resulted in a decrease in the monomer/dimer ratio, followed by re-equilibration in the dark. Calculation of the solvent-accessible surface area and the Conolly surfaces of the LOV1 dimers present in the crystal structure support the experimental observation that no mononomers are detected in the native state. A model is presented that accounts for a blue-light-driven change in the quaternary structure of the LOV1 domain and gives hints to the molecular basis of light activation and regulation in LOV-containing proteins.*

Introduction

Phototropins are flavoprotein photoreceptors that mediate a variety of physiological processes in plants.[1–3] Whereas in most species two phototropins, phot1 and phot2 regulate the response to light, the green alga *Chlamydomonas reinhardtii* contains only one photoreceptor, designated phot. Phototropins are serine/threonine protein kinases that undergo autophosphorylation of the C-terminal kinase domain upon irradiation with blue light (Figure 1).[4–6] The N-terminal region contains two similar motifs that belong to the large and diverse superfamily of **P**ER/**A**RNT/**S**IM (PAS) proteins.[7] Because these PAS domains are regulated by external signals, such as light, oxygen, or voltage they are termed LOV1 and LOV2 (Figure 1).[5] Both LOV domains of the phototropins serve as binding pockets for the chromophore FMN, and are directly involved in light sensing.[8–9] The LOV2 domain is C-terminally linked by a highly conserved α helix (Jα) to the kinase domain (Figure 1).

The activation of phototropins is assumed to occur in a series of events beginning with the absorption of blue light by the LOV domains. In the dark or ground state, the phototropin receptor remains unphosphorylated and inactive. After absorption of light, the LOV domains go through a photocycle that is characterized by a series of transient photointermediates.[11,12,15] In the photocycle two electronic excited states and one metastable thermal intermediate have been kinetically resolved.[11,15] The metastable thermal intermediate, LOV-390 contains FMN covalently bound to the thiol group of the reactive cysteine (Cys57 in LOV1 from *C. reinhardtii*) via the C(4a) position of the isoalloxazine ring.[9,16–18] Subsequently, the phototro-

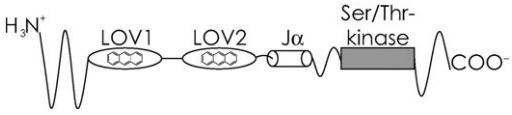

Figure 1. Schematic drawing of the phototropin from *C. reinhardtii* (749 amino acids). The light-sensing LOV domains, each of which binds FMN are indicated. The serine/threonine kinase domain is shown in gray. A conserved α helix at the C-terminal position of LOV2 (Jα) is also shown. Displacement of this helix in response to LOV2 photoexcitation has been proposed to result in the activation of the C-terminal kinase domain.[19]

[a] *R. J. Kutta, Prof. Dr. B. Dick*
Institut für Physikalische und Theoretische Chemie
Universität Regensburg, Universitätsstrasse 31
93053 Regensburg (Germany)
Fax: (+49) 941-943-4488
E-mail: bernhard.dick@chemie.uni-regensburg.de

[b] *Dr. E. S. A. Hofinger, Dr. H. Preuss, Prof. Dr. G. Bernhardt*
Institut für Pharmazie, Universität Regensburg
Universitätsstrasse 31, 93053 Regensburg (Germany)
Fax: (+49) 941-943-4488
E-mail: guenther.bernhardt@chemie.uni-regensburg.de

Supporting information for this article is available on the WWW under http://www.chembiochem.org or from the author.

pin is activated by autophosphorylation of the kinase domain, and mediates the transfer of the signal downstream.[35,36]

For many LOV domains it has been shown that they undergo structural changes in the proximity of the chromophore during their photocycle. In prokaryotes the LOV light-sensing domain is coupled to diverse effector domains.[22–23] Although the exact role of the LOV domains in the activation cycle of the kinase is not fully understood, it is assumed that after light sensing, the highly conserved α-helical region (Jα) is released from the surface of LOV2.[19] This displacement is hypothesized to lead to an activation of the C-terminal kinase domain, which in turn results in autophosphorylation of the photoreceptor protein.[19–20] This suggestion was put into question, when it was observed that the Jα linker is needed neither for the LOV2-kinase interaction, nor for the light-driven phosphorylation of a substrate.[21] LOV1 acts as an attenuator of the photoactivation, possibly because of a stereochemical blocking of the interactions between LOV2 domain and kinase domain independently of the photoreaction of LOV1.[21]

So far it is not known how the light-induced reactions that are centered on a LOV domain are transmitted to the effector domains, whether this occurs by the same molecular mechanism in all cases, and whether the LOV domains always interact with other domains in the same orientation. The latter question arises because in phot1-LOV2 of *Avena sativa* the central β-scaffold has been demonstrated to participate in interdomain communication while making contact with the Jα linker.[19–20] However, in bacterial LOV proteins only one LOV domain is present, whereas phot contains two such motifs organized in tandem.[22–23] Hence, a LOV–LOV interaction might not be necessary for the function, or at least in bacteria, it occurs between LOV domains of different protein molecules.

It was observed that the LOV2 domain has a higher photocycle quantum yield than LOV1.[10] Therefore, LOV2 acts as the basic light-sensing domain and triggers the phot1 and phot2 kinase activity. LOV1 is supposed to play a regulatory role.[24] A comparison of the amino acid sequences of bacterial LOV domains with LOV1 and LOV2 of phot proteins revealed that in general, bacterial LOV domains have intermediate characteristics between LOV1 and LOV2.[23]

The tendency of LOV domains to form dimers has been noticed previously.[25–30] Salomon et al. showed by using size-exclusion chromatography that phot1-LOV1 dimerizes, but LOV2 stays monomeric.[25] In this work the authors suggested that LOV1 is responsible for phot dimerization, which would provide a possible functional role for the tandem organization of LOV domains in phot proteins.[25] An increase in volume by a factor of about 1.8 during light activation of an extended phot1-LOV2 construct, which was observed by a laser-induced thermal grating technique has been interpreted as a transient dimerization in the time range of 300 μs.[26] Using small-angle X-ray scattering (SAXS) Nakasako et al. reported on the detection of dimeric states for the LOV domain of FKF1 and phot LOV1 domains.[27–28] The SAXS experiments showed that phot1-LOV2 is dimeric, whereas phot2-LOV2 is monomeric.[25–26] The latter results are at variance with those reported by Salomon et al. and Nakasone et al.[25–26] Another example for LOV–LOV dimerization is the LOV domain of WC-1 from *Neurospora*, which showed homodimerization in vitro.[29] Recently, dimerization and interdomain interactions were observed in the isolated YtvA-LOV domain by size-exclusion chromatography.[30] Circular dichroism (CD) spectroscopy measurements showed a central distortion in the β scaffold of the LOV domain. These data led to the proposal of a common surface for LOV–LOV and intraprotein interaction that involves the central β scaffold.[30]

Apparently, LOV–LOV interactions that lead to dimers are a common feature of many LOV domains, but their role in the signaling cascade still needs to be uncovered. In particular, it should be investigated whether this interaction is modulated by the photochemistry of the LOV domains. To gain insight into the role of the LOV1 domain in the light-induced activation of phototropins, we investigated isolated LOV1 domains from *C. reinhardtii* with respect to oligomerization, and investigated whether the LOV–LOV interaction is correlated to the light sensitivity of these domains.

Results and Discussion

Recovery of the dark-state after "fast bleaching"

Immediately after strong bleaching with a high-power LED at 460 nm, the absorption spectrum of the sample in the range $\lambda > 300$ nm consists of a single broad band with maximum at 390 nm. This has been previously assigned to the adduct of Cys57 to FMN.[9,16–18] Figure 2A displays examples from a sequence of 150 spectra that were measured at intervals of 20 s during the recovery of the system in the dark. The final spectrum, which corresponds to a delay time of 3000 s is identical to the spectrum taken before irradiation. This data set has been decomposed into the superposition of two spectra $S_j(\lambda)$ and two concentration profiles $c_j(t)$ according to Equation (1):

$$A(\lambda,t) = S_1(\lambda)c_1(t) + S_2(\lambda)c_2(t) \quad (1)$$

(for details see the Supporting Information). The resulting spectra are shown in the Figure 2B, and the concentration profiles are shown in Figure 3A. The sum of these, which is shown as curve $(c_1 + c_2)$ in Figure 3A, deviates from a constant value by less than ±1% over the whole temporal range. Hence, only the concentration profile $c_1(t)$ assigned to the adduct species is analyzed in the following.

The residuals of a single exponential decay fit to $c_1(t)$ results in the line (*s*) of Figure 3B. The deviations are much larger than the noise, hence the decay can definitely not be described properly by a single exponential. A double exponential function leads to a significantly better fit (Figure 3B, d). Incidentally, the fit finds almost identical amplitudes for the two decay components. A model that accounts for such behavior would be a 1:1 mixture of two structural isomers of the LOV1 protein, one with a short recovery time and the other with a long recovery time. An alternative explanation is the existence of dimers in which the two monomers occupy nonequivalent sites. This would in particular account for the equal ampli-

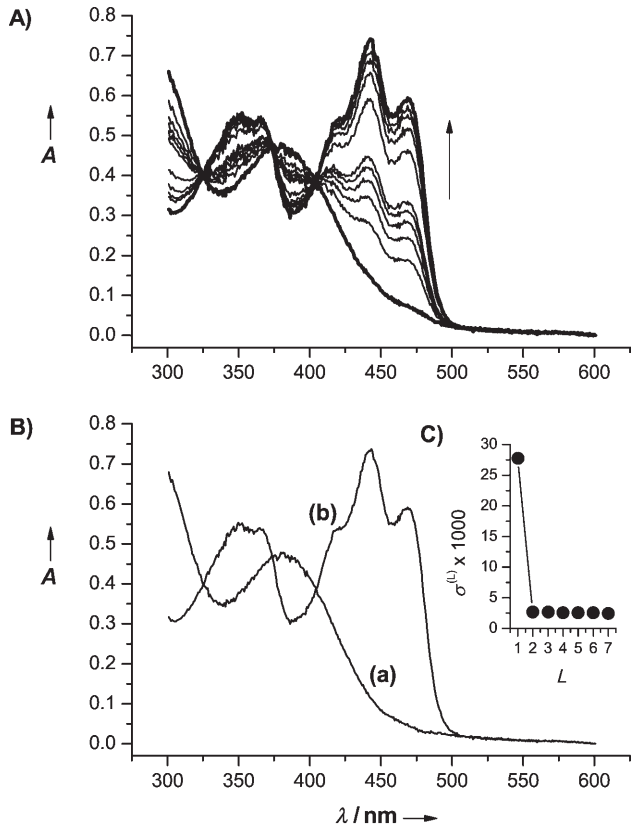

Figure 2. A) Sequence of spectra measured at increasing delay times following irradiation of LOV1 for 1 s with a strong blue-light emitting LED. Spectra were measured at intervals of 20 s for a total duration of 3000 s. The integration time obtained by measuring a single spectrum was 25 ms; this short period of irradiation with white light was found not to affect adduct formation during the registration of a single spectrum. In addition, we made sure that an interval of 20 s between the recordings of subsequent spectra had no effect. Only the spectra at delays 0, 20, 40, 60, 80, 100, 300, 500, 700, 900, and 3000 s are shown. B) Spectra of the photoadduct (a) and the dark form (b) of LOV1. C) Standard deviation between the data and a reconstruction with an increasing number *L* of principal components.

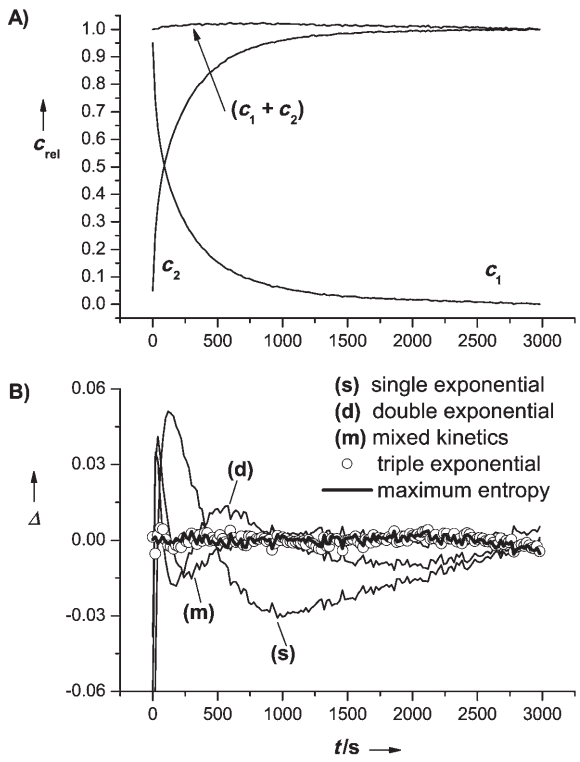

Figure 3. A) Decay of the adduct fraction (c_1) and rise of the dark form (c_2). The sum of both concentrations is constant within ±1%. B) Residuals (Δ) of the fits of several model functions to the decay curve of the adduct.

tudes. A fit of similar quality is, however, observed with the function [Eq. (2)]:

$$c(t) = \frac{k_1 c_0}{\exp(k_1 t)(k_1 + k_2 c_0) - k_2 c_0} \quad (2)$$

This function is the solution of the differential Equation (3):

$$\frac{dc}{dt} = -k_1 c - k_2 c^2 \quad (3)$$

which is the superposition of a monomolecular and a bimolecular decay process. Although a double exponential function as well as the mixed kinetics of Equation (4) yield a better fit than a single exponential, the residuals still show a systematic deviation from zero that exceeds the noise significantly (Figure 3B, m). One might hence ask whether the system is inhomogeneous, that is, whether it contains molecules that represent a whole distribution of rate constants $p(k)$ that lead to the apparent decay function:

$$c(t) = \int_0^8 dk p(k) \exp(-kt) \quad (4)$$

The inversion of this Laplace transform with the aim of obtaining the distribution function $p(k)$ is a classical ill-posed problem, but can be solved by the maximum entropy method.[37,38] The result is shown in Figure 4, and the corresponding residuals of the fit are shown in Figure 3B (○), and are indistinguisha-

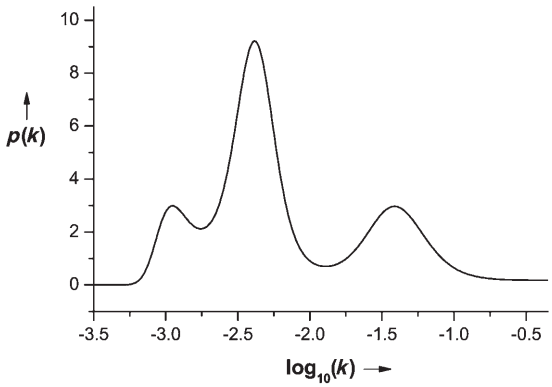

Figure 4. Laplace inverse of the decay curve of the adduct obtained with the maximum entropy method. The amplitude $p(k)$ is plotted versus the logarithm of the rate constant, *k*. Three maxima occur at the rate constants 3.84×10^{-2}, 4.11×10^{-3}, and 1.21×10^{-3} s^{-1}. These correspond to lifetimes of 26, 244, and 823 s.

ble from the noise. The distribution function has three maxima that correspond to decay times of 26, 244, and 823 s. This suggests that a three-exponential decay function might also yield a satisfactory fit. Indeed, such a fit is almost as good as the result from the inverse Laplace transform by maximum entropy (residuals in Figure 3B). We conclude, that the thermal decay of the photoadduct back to the dark form indicates that the system is inhomogeneous. A fit with residuals at the noise level requires at least three exponentially decaying components. However, if we allow for some amount of systematic error in the measurement, a double-exponential fit or a mixed kinetic model might also be acceptable. These observations point to the possibility that the sample contains dimers or aggregates of LOV1 domains, and that bimolecular reactions might be involved in the equilibration of the sample in the dark. However, no dependence of the decay curves on the concentration of LOV domains was observed in the range from $OD_{447\,nm} = 0.2$ to 1.2.

SEC of the natural LOV (LOV1-wt) domain under native conditions

SEC analysis of a pure sample of LOV1 showed a distinct peak at 91 min (corresponding to a molecular mass of 30 kDa) and a broad peak at about 66 min with a shoulder at about 60 min (Figure 5). For the 66 min peak a molecular mass of >200 kDa was calculated. This demonstrates that LOV1 forms dimers (30 kDa) and higher oligomers (>200 kDa). No peaks that corresponded to monomers, trimers or oligomers up to tetradecamers were detected. To investigate whether dimers and oligomers exist at equilibrium, the peaks were fractionated, concentrated, and re-loaded onto the column. The chromatograms of both fractionated samples showed a size distribution of LOV1 that was very similar to the initial one (Figure 5). This demonstrates that in the dark the LOV1 domain stays in equilibrium between dimers and higher aggregates. An increase in the ionic strength of the eluent shifted the equilibrium towards the aggregates, which is very unusual.

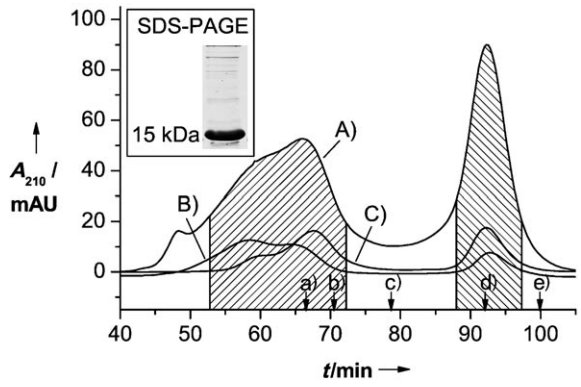

Figure 5. Equilibrium between LOV-wt dimers and higher aggregates under native conditions. Elution profiles were obtained from the Superdex 200 pg column. The peak positions of the standard proteins used for calibration are indicated by arrows as follows: a) β amylase (200 kDa); b) alcohol dehydrogenase (150 kDa); c) albumin (66 kDa); d) carboanhydrase (29 kDa); e) cytochrom c (12.4 kDa). The sample (1 mL, 0.92 mg mL^{-1}) was loaded on the column, and the fractions were pooled according to the elution profile (hatched areas) and concentrated in centrifugal filter devices. The mobile phase was sodium phosphate buffer (10 mM, pH 8.0) supplemented with NaCl (10 mM). The concentrated fractions that contained high or low-molecular weight compounds were reanalyzed. A) Chromatogram corresponds to the initial LOV1-wt sample; B) the result of the fractionated high-molecular peak from the initial run; C) the result of the fractionated low-molecular-weight peak from the initial run; inset: lane from the SDS gel showing only monomers in the native LOV1 sample (without cross-linking).

Cross-linking in the dark

For analysis of the equilibrium, cross-linking with glutardialdehyde was performed because analytical ultracentrifugation is inadequate on the required time scale. Electron paramagnetic resonance spectroscopy requires unpaired electrons, which are not present in LOV1 and would require labeling of the protein, and which might affect interactions.

Obviously, the LOV1 domain exhibits a tendency for oligomerization. One set of samples was illuminated for different periods of time with blue light before the cross-linking reaction. A second set of samples was illuminated with blue light for a constant period of time and was incubated in the dark for different periods of time before being cross-linked. This analysis was not feasible with SEC because the time required for elution exceeds the thermal recovery time of the dark state.

To "freeze" the association/dissociation equilibrium of LOV1, ε-amino groups on the surface of a monomer (nine lysines) were covalently cross-linked by glutardialdehyde as described previously.[31] With references, which were not subjected to the cross-linking procedure, we proved that sample preparation (dialysis, vacuum concentration and solubilization) did not cause aggregation. In the absence of the cross-linking agents, only monomers that corresponded to a M_W of approximately 15 kDa were detected by SDS-PAGE (Figure 5, inset). As a reference to the blue-light effect, a sample of pure LOV1 was cross-linked in the dark. The SDS-PAGE showed two bands that corresponded to about 15 kDa (monomer) and 30 kDa (dimer), respectively (Figure 6, lane B). To account for a potential loss of protein associated with the sample preparation for SDS-PAGE, BSA (Figure 6A and B, 66 and 50 kDa bands) was added as an

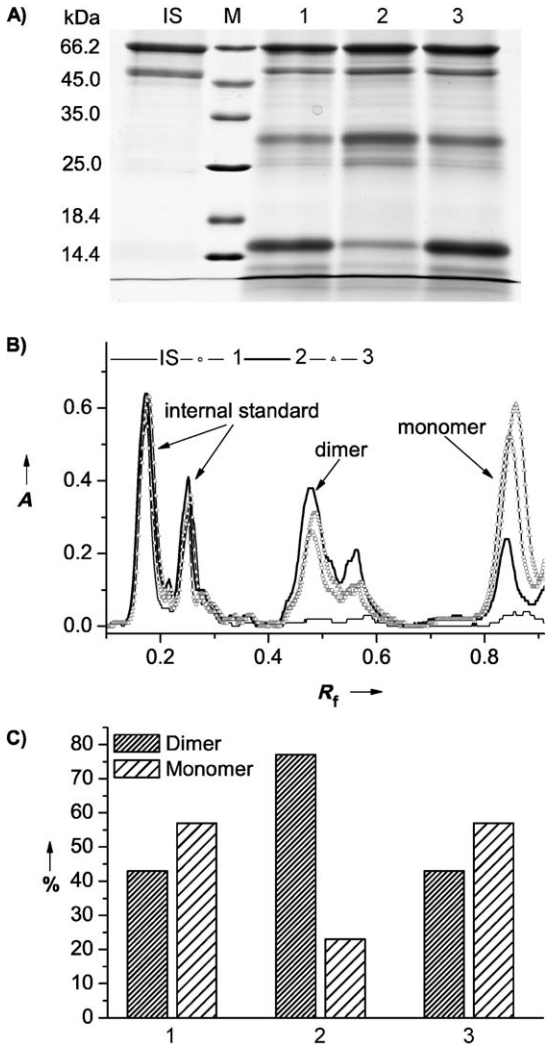

Figure 6. Blue-light induced changes of the monomer/dimer ratio in LOV1-wt. The concentration of LOV1-wt was 55 μM. A) Polyacrylamide gel (15%); lane IS: internal standard (10 μL; 10 μg μL^{-1} bovine albumin: 66 kDa); lane M: molecular-weight marker; lane 1: sample cross-linked in the dark before SDS-PAGE; lane 2: exposed to blue LEDs for 3 min before cross-linking and SDS-PAGE; lane 3: exposed to blue LEDs for 3 min, incubated for 40 min in the dark, and then cross-linked before SDS-PAGE. B) Corresponding densitometer plots of lanes IS and 1–3. C) Data of the experiments with LOV1-wt. The values of the areas for the dimers and the monomers are shown in lanes 1–3.

internal standard after cross-linking. As is obvious from Figure 6A and B, the BSA contained an impurity. However, this impurity did not interfere with the analytes (monomers, dimers). Additional bands on the gel might represent small amounts of proteolytic fragments, because rather than a protease inhibitor cocktail (containing peptides), only PMSF was used to prevent interference with SDS-PAGE.

Although the recoveries of the samples differed slightly, the sum of the monomers and dimers was constant, with respect to the amount of the internal standard (BSA; Figure 6A and B).

The yield of the cross-linking reaction strongly depended both on the concentration of glutardialdehyde and on the reaction time. The incubation period was kept constant at 2 min, and the glutardialdehyde concentration was varied between 0 and 5.5%. In the range between 0.2 and 3.5% of glutardialdehyde, the monomer/dimer ratio remained constant at a value of about 1.3. In no case were species other than monomers and dimers detected. For quantitative analysis of the densitometric plots, all peaks were numerically fitted with Gaussian functions, which enables the determination of the areas of overlapping peaks. The amounts of monomers and dimers were calculated by the integrated optical density of the peak, which was correlated to the integrated optical density of the internal standard. In contrast to the SEC analysis, which showed only dimers and oligomers of high molecular weight, after cross-linking both monomers and dimers were identified.

Effect of blue light exposure on the monomer/dimer ratio

To investigate the effect of blue light on LOV1, a sample was illuminated with intensive LEDs for 3 min and cross-linked immediately. Another sample was also illuminated for 3 min, but was cross-linked after an incubation time of 40 min in the dark (Figure 6). In comparison to the dark state, the ratio of monomers to dimers decreased from 1.3 to about 0.3 after exposure to blue light (Figure 6, lane C). When LOV1 was incubated in the dark for 40 min after light exposure, the monomer/dimer ratio of the dark state was recovered (Figure 6, lane D).

These experiments showed that the influence of light on the association state of LOV1 is reversible. Apparently, the formation of the adduct-state results in structural changes on the protein surface, which influence the intermolecular interactions of the LOV1 domain.

Kinetics of monomer/dimer ratio during irradiation and relaxation in the dark

To assess the time required to reach the light-adapted state, the time of light exposure before cross-linking was varied. Samples of LOV1 were irradiated with blue light for different periods of time (0.5, 1, 2, and 3 min) and immediately cross-linked (Figure 7). As a control an identical sample was cross-linked in the dark. An exposure time of 0.5 min already resulted in a significant decrease in the monomer/dimer ratio compared to the dark state. Before exposure, the amount of dimers was about 40%. Immediately after 0.5 min of exposure to light the amount of dimers increased to about 75%. This value remained constant after longer exposure times (Figure 8A).

Furthermore, the incubation period in the dark after irradiation with blue light for 2 min and before cross-linking, was varied. Incubation times of 2, 6, 10, 20, 30, and 40 min were selected. As a reference, an identical sample was cross-linked without exposure to light (Figure 7B). After an incubation period of 2 min the monomer/dimer ratio was comparable to the one detected directly after illumination, that is, there were about 70% dimers. By contrast, upon longer incubation times the amount of monomers increased significantly, and the monomer/dimer ratio returned to that of the dark state. Figure 8B illustrates this phenomenon in a plot of the amounts of monomers and dimers versus time. The time constant for this pro-

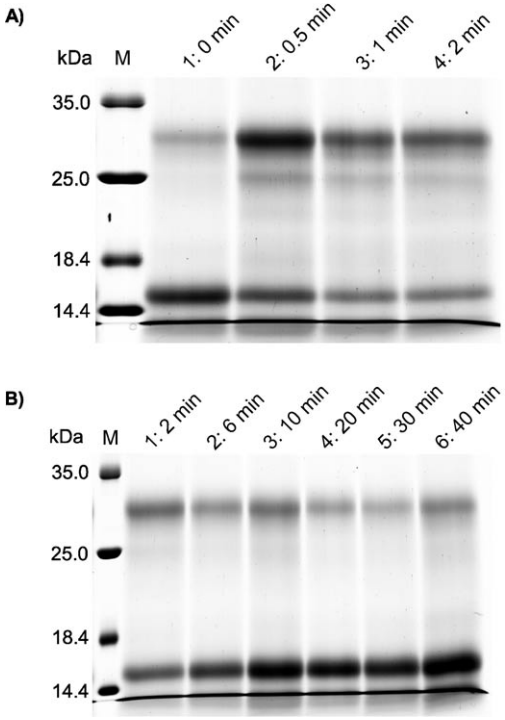

Figure 7. A) Effect of exposure time on the monomer/dimer ratio. The concentration of LOV1-wt was 55 μM. The following exposure times before cross-linking were chosen: lane 1: cross-linked in the dark; lane 2: 0.5 min; lane 3: 1 min; lane 4: 2 min; lane M: molecular-weight marker. B) Influence of incubation time on the monomer/dimer ratio. The concentration of LOV1-wt was 55 μM. The following incubation times in the dark after a constant exposure time of 2 min, and before cross-linking were used: lane 1: 2 min; lane 2: 6 min; lane 3: 10 min; lane 4: 20 min; lane 5: 30 min; lane 6: 40 min.

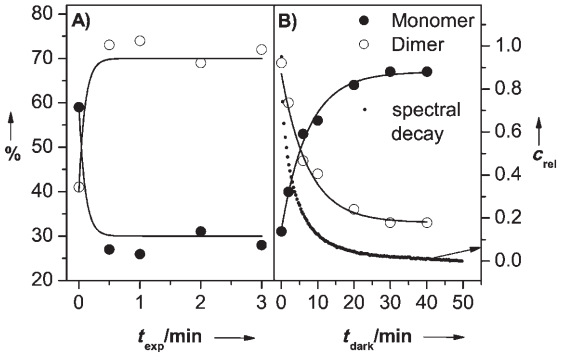

Figure 8. Effect of exposure time on the monomer/dimer ratio, A) determined by fitting the peaks in the densitometer plots with Gaussian functions, and B) the time in the dark after 3 min of exposure. The fitted exponential curves yield a time constant of about 7 min. The dots show the spectral decay of the fraction of adduct, which is in the same order of magnitude as the decay of the monomer/dimer ratio in the dark after an exposure time of 3 min. The concentration of LOV1-wt was 55 μM.

cess is about 7 min. The time constant of the spectral recovery is about 200 s. If one considers the experimental time resolution of the cross-linking experiments of about 2 min, both time constants are of comparable magnitude.

Model of a LOV1 dimer

SEC analysis under native conditions showed that LOV1 exists mainly as a dimer in the dark. SDS-PAGE experiments with and without cross-linking confirmed that these dimers are not covalently bound. To visualize the quaternary structure, an analysis on the basis of the X-ray crystal structure of the LOV1 domain from *C. reinhardtii*, which was solved by Fedorov et al.[18] (PDB ID code: 1N9L) was performed. For this purpose, the monomeric structure was expanded in its P 65 2 2 symmetry in the crystal, which yielded a circular oligomeric structure. An enlargement of the neighboring space of a single LOV1 domain within the crystal reveals that a single domain (a) is surrounded by four neighboring domains (b–e), which are in direct contact (Figure 9A). These four different kinds of dimers were analyzed in more detail by calculating the solvent-accessible surface area (SASA) of each dimer and of a single domain by subtraction of the double SASA of a single domain by the corresponding SASA of the dimer; this gave an estimate of the total contact area within each type of dimer. The dimer [a|b] showed the largest contact area. The Conolly surface of the LOV1 domain was calculated and revealed a lipophilic area in the left bay of the domain (Figure 9B, brown region), which protrudes into the direction of an area with higher hydrophilic-

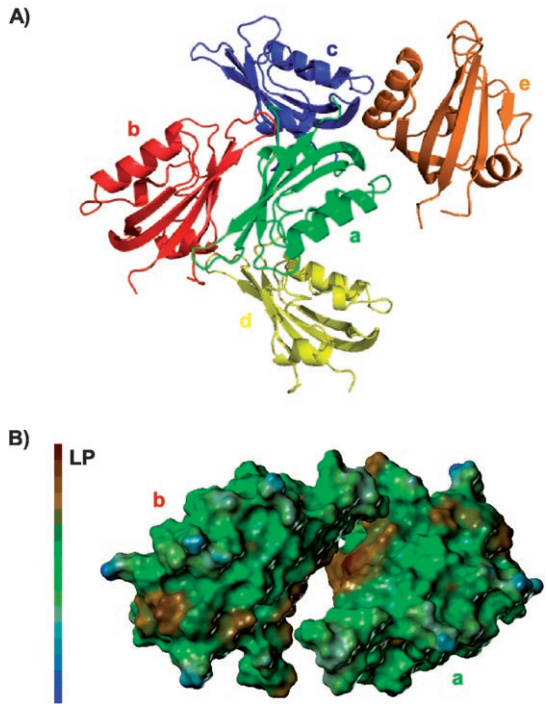

Figure 9. Analysis of the quaternary structure on the basis of the X-ray crystal structure of the LOV1 domain from *C. reinhardtii* (PDB ID code: 1N9L). A) Neighboring space of a single LOV1 domain within the crystal (crystallized in P 65 2 2 symmetry) reveals that a single domain (a) is surrounded by four other domains (b–d) and is in direct contact with them. The dimer [a|b] shows the largest contact area (calculated by SASA); this suggests that this type of dimer is most stable. B) Calculated Conolly surfaces of the LOV1 domains in the [a|b] dimer. The lipophilic potential shows a lipophilic area (brown region) in the left bay of the domain, which protrudes in the direction of an area with higher hydrophilicity (green region). In the dimer [a|b] both lipophilic surfaces fit very well sterically.

ity (Figure 9B, green region). In the dimer [a|b] both lipophilic surfaces point to each other and fit very well sterically. Therefore, we assume the dimer [a|b] predominates in solution.

Conclusions

Kinetic measurements showed that the thermal back-reaction from the photoadduct to the dark state is inhomogeneous. A possible reason for this could be the coexistence of monomers, dimers, and higher aggregates. In this case bimolecular reactions may participate in adjusting the equilibrium in the dark. Analysis of LOV1 by SEC showed a mixture of dimers and higher aggregates (larger than tetradecamers). These oligomers were shown to exist at equilibrium, which can be shifted to the higher aggregates with an increasing ionic strength in the eluent.

Cross-linking of LOV1 in the dark and subsequent SDS-PAGE showed that the dimers that were identified in the SEC are bound by noncovalent interactions. Without cross-linking, only monomers could be observed by SDS-PAGE. The higher aggregates that were observed in the SEC were not detected by SDS-PAGE. Apparently, the probability of cross-linking of such higher aggregates is too low. Furthermore, monomers were detected, which were not seen in the SEC.

The observation of monomers after SDS-PAGE indicates that cross-linking is not complete. Because no monomers exist in the native state, the increase of the dimer fraction following excitation with blue light can not be due to dimer formation from monomers. One plausible explanation is that the dimers, even those that are obviously present as subunits in the higher aggregates, undergo a conformational change in the photoexcited state that strongly increases their cross-linking yield. This might happen because the distances between the lysines decrease in the photoexcited state so that the cross-linking reaction is more probable (see figure in the graphical abstract). Such a photoinduced increase of the LOV–LOV interaction might be important for signal transduction if, as suggested,[30] the autophosphorylation of phot is in fact a mutual cross-phosphorylation of a pair of phot proteins.

In summary, our observations indicate a light-induced interaction between the LOV1 domains from *C. reinhardtii*. Blue light induces the formation of the adduct state within the protein, and this adduct formation then forces the protein into a conformation in which the interaction between two LOV1 domains is strongly increased. This kind of blue-light-driven interaction between LOV1 domains might also occur in the full-length protein phototropin, and might play a role in the signal transduction pathway.

Experimental Section

Materials: Bacto tryptone, agar and yeast extract were purchased from Becton, Dickinson and Company (Sparks, USA). PMSF was bought from Roth (Karlsruhe, Germany) and the molecular weight standards for SDS-PAGE were purchased from Peqlab (Erlangen, Germany). Water was purified by a Milli-Q system (Millipore, Eschborn, Germany). All other chemicals were of analytical grade and were obtained either from Merck or from Sigma–Aldrich.

LOV1 expression and purification: The gene fragment that encoded the FMN-binding LOV1-wt domain (amino acids 16–133) was cloned into the *E. coli* expression vector Hispx2 between the EcoRI and HindIII sites in such a way that the protein carried one Met, twelve His, one Glu, and one Phe that were derived from the vector sequence at the N-terminal end. (The Hispx2 vector was produced by cutting off the sequence that coded for the maltose-binding protein out of the pMal-p2x vector (New England Biolabs, Frankfurt, Germany) in a first step, and then inserting a sequence that encoded 10×His.) The protein was expressed in *E. coli* strain BL21 (New England Biolabs, Frankfurt, Germany) and purified by a Ni-NTA column (Qiagen, Hilden, Germany) as described previously.[11] After purification, LOV1 was dialyzed against sodium phosphate buffer (10 mM, pH 8.0) that contained NaCl (10 mM) and PMSF (0.1 mM).

UV/Vis spectroscopy: For all bleaching experiments LOV1 was diluted in sodium phosphate (10 mM, pH 8.0) that contained NaCl (10 mM) to yield a protein concentration of 0.85 mg mL^{-1}. LOV1 concentrations were determined by measuring the absorption at 447 nm by using the extinction coefficient $\varepsilon_{447} = 12\,500\ \mathrm{L\,mol^{-1}\,cm^{-1}}$ of free FMN. This determination was based on the assumption of identical extinction coefficients for free and LOV1-bound FMN. For photobleaching, the samples were irradiated for 1 s with intense blue light LEDs (Luxeon® III Emitter Königsblau, Lumileds Lighting, San Jose, USA) with an emission maximum of 460 nm and a width at half height of 20 nm. LEDs were positioned on both sides of the cuvette. Immediately after bleaching, time sequences of spectra were collected in the dark every 20 s for an overall time interval of 3000 s. The shutter of the diode array was opened for only 25 ms, which is too short a period of irradiation time with white light to affect adduct formation during the registration of a single spectrum. In addition, we made sure that an interval of 20 s between the recordings of subsequent spectra had no effect. Cuvettes were maintained at a temperature of 20 °C during the measurements. Absorption spectra were measured with a Lambda 9 spectrophotometer (Perkin–Elmer), and time sequences of the spectra were recorded with a Specord S100B diode array spectrometer (Analytik Jena, Jena, Germany).

Size-exclusion chromatography (SEC): Prior to the separation of LOV1, a Superdex 200 pg 16/60 column (GE Healthcare, Uppsala, Sweden) was equilibrated with sodium phosphate buffer (10 mM, pH 8.0) supplemented with NaCl (10 mM). Calibration was performed with gel filtration by using molecular weight markers of 12 400–200 000 Da (Sigma–Aldrich, Munich, Germany). After calibration Ni-IMAC purified LOV1 was separated by SEC. The LOV1 sample (1 mL) with a concentration of 0.84 mg mL^{-1} was applied to the column and separation was performed at a flow rate of 1 mL min^{-1} and a detector wavelength of 280 nm by using an Äkta Purifier FPLC system (GE Healthcare, Uppsala, Sweden). All SEC experiments with LOV1 were performed in the dark at 8–9 °C. Fractions were pooled according to the elution profile and were concentrated in centrifugal filter devices (MWCO 5000, Amicon Ultra-5, Millipore, Eschborn, Germany). The concentrated fractions that contained high or low-molecular-weight compounds, were then reanalyzed by SEC. Fractions were separately applied to the Superdex 200 pg 16/60 column, and elution profiles were detected as described above.

Cross-linking with glutardialdehyde: Cross-linking with glutardialdehyde was essentially performed as described in ref. [31, 33]. Brief-

ly, sodium phosphate (421 μL, pH 8.0; 10 mM) that contained NaCl (10 mM) was mixed with 2.5% (*v/v*) aq. glutardialdehyde solution (50 μL). After 30 s, protein solution (0.85 μg mL^{-1}; 29 μL) was injected, and the mixture was shaken vigorously for 2 min. The reaction was stopped by addition of $NaBH_4$ (ca. 10 mg) and shaken for 20 min to assure complete reduction of excess glutardialdehyde. Concentrated H_3PO_4 (30 μL) was added in three portions. After addition of SDS solution (10%, *w/v*; 100 μL) the samples were dialyzed (MWCO 10000 Da) against SDS (0.2%, *w/v*) at 60 °C. Samples were dried, overnight, in a speedvac (Savant speedvac Plus SC110A; Divebid, Cambridge, USA) at low temperature before they were dissolved in water (12 μL) and Laemmli buffer (3 μL) for subsequent SDS-PAGE analysis.

SDS-PAGE: SDS-PAGE was performed as described in ref [34]. Proteins were separated in 12 or 15% polyacrylamide gels by using a PerfectBlue™ gel electrophoresis system Twin S (Peqlab, Erlangen, Germany). All samples were heated for 3 min at 100 °C before they were loaded onto the gel. The gels were scanned and analyzed in a GS-710 Imaging Densitometer by using Quantity One quantification software, version 4.0.3 (Bio-Rad, Munich, Germany). For quantitative evaluation of protein peaks the fitting routines in the program Origin (OriginLab Corporation, Northampton, USA) were used.

Calculation of LOV1 surfaces and visualisation of dimer formation: The vicinity of a LOV1 monomer within the crystal (Figure 9) was analyzed with the software package PyMOL[40] by using the symmetry information within the PDB file 1N9L. Solvent-accessible surface areas were calculated with VEGA ZZ 2.1.0.[39]

Connolly surfaces were calculated by using Sybyl version 7.1 (Tripos, St. Louis, USA). Inorganic ions and water molecules were excluded and a radius of 1.4 Å was chosen for the contact molecule. In accordance with the distribution of lipophilic residues and the electrostatic potential on the Connolly surface, the proposed protein dimers were fitted manually.

Acknowledgements

We thank Prof. Dr. Peter Hegemann and his group at HU Berlin for providing us with the plasmids. The work was supported by the Deutsche Forschungsgemeinschaft (DFG) in the Graduate College, GK 640, "sensory photoreceptors in natural and artificial systems".

Keywords: *Chlamydomonas reinhardtii* · photochemistry · photoreceptors · phototropin · protein structures

[1] W. Briggs, C. Beck, A. Cashmore, J. Christie, J. Hughes, J. Jarillo, T. Kagawa, H. Kanegae, E. Liscum, A. Nagatani, K. Okada, M. Salomon, W. Rüdiger, T. Sakai, M. Takano, M. Wada, J. Watson, *Plant Cell* **2001**, *13*, 993–997.
[2] W. R. Briggs, J. M. Christie, *Trends Plant Sci.* **2002**, *7*, 204–210.
[3] R. Banerjee, A. Batschauer, *Planta* **2005**, *220*, 498–502.
[4] J. M. Christie, P. Reymond, G. K. Powell, P. Bernasconi, A. A. Raibekas, E. Liscum, W. R. Briggs, *Science* **1998**, *282*, 1698–1701.
[5] E. Huala, P. W. Oeller, E. Liscum, I.-S. Han, E. Larsen, W. R. Briggs, *Science* **1997**, *278*, 2120–2123.
[6] E. Knieb, M. Salomon, W. Rüdiger, *Planta* **2004**, *218*, 843–851.
[7] B. L. Taylor, I. B. Zhulin, *Microbiol. Mol. Biol. Rev.* **1999**, *63*, 479–506.
[8] J. M. Christie, M. Salomon, K. Nozue, M. Wada, W. R. Briggs, *Proc. Natl. Acad. Sci. USA* **1999**, *96*, 8779–8783.
[9] M. Salomon, J. M. Christie, E. Knieb, U. Lempert, W. R. Briggs, *Biochemistry* **2000**, *39*, 9401–9410.
[10] M. Kasahara, T. E. Swartz, M. A. Olney, A. Onodera, N. Mochizuki, H. Fukuzawa, E. Asamizu, S. Tabata, H. Kanegae, M. Takano, J. M. Christie, A. Nagatani, W. R. Briggs, *Plant Physiol.* **2002**, *129*, 762–773.
[11] T. Kottke, J. Heberle, D. Hehn, B. Dick, P. Hegemann, *Biophys. J.* **2003**, *84*, 1192–1201.
[12] A. Losi, E. Polverini, B. Quest, W. Gärtner, *Biophys. J.* **2002**, *82*, 2627–2634.
[13] T. Imaizumi, H. G. Tran, T. E. Swartz, W. R. Briggs, S. A. Kay, *Nature* **2003**, *426*, 302–306.
[14] C. Schwerdtfeger, H. Linden, *EMBO J.* **2003**, *22*, 4846–4855.
[15] T. E. Swartz, S. B. Corchnoy, J. M. Christie, J. W. Lewis, I. Szundi, W. R. Briggs, R. A. Bogomolni, *J. Biol. Chem.* **2001**, *276*, 36493–36500.
[16] M. Salomon, W. Eisenreich, H. Dürr, E. Schleicher, E. Knieb, V. Massey, W. Rüdiger, F. Müller, A. Bacher, G. Richter, *Proc. Natl. Acad. Sci. USA* **2001**, *98*, 12357–12361.
[17] S. Crosson, K. Moffat, *Plant Cell* **2002**, *14*, 1067–1075.
[18] R. Fedorov, I. Schlichting, E. Hartmann, T. Domratcheva, M. Fuhrmann, P. Hegemann, *Biophys. J.* **2003**, *84*, 2474–2482.
[19] S. M. Harper, J. M. Christie, K. H. Gardner, *Biochemistry* **2004**, *43*, 16184–16192.
[20] S. M. Harper, L. C. Neil, I. J. Day, P. J. Hore, K. H. Gardner, *J. Am. Chem. Soc.* **2004**, *126*, 3390–3391.
[21] D. Matsuoka, S. Tokutomi, *Proc. Natl. Acad. Sci. USA* **2005**, *102*, 13337–13342.
[22] S. Crosson, S. Rajagopal, K. Moffat, *Biochemistry* **2003**, *42*, 2–10.
[23] A. Losi, *Photochem. Photobiol. Sci.* **2004**, *3*, 566–574.
[24] J. M. Christie, T. E. Swartz, R. A. Bogomolni, W. R. Briggs, *Plant J.* **2002**, *32*, 205–219.
[25] M. Salomon, U. Lempert, W. Rüdiger, *FEBS Lett.* **2004**, *572*, 8–10.
[26] Y. Nakasone, T. Eitoku, D. Matsuoka, S. Tokutomi, M. Terazima, *Biophys. J.* **2006**, *91*, 645–653.
[27] M. Nakasako, T. Iwata, D. Matsuoka, S. Tokutomi, *Biochemistry* **2004**, *43*, 14881–14890.
[28] M. Nakasako, D. Matsuoka, K. Zikihara, S. Tokutomi, *FEBS Lett.* **2005**, *579*, 1067–1071.
[29] P. Ballario, C. Talora, D. Galli, H. Linden, G. Macino, *Mol. Microbiol.* **1998**, *29*, 719–729.
[30] V. Buttani, A. Losi, T. Eggert, U. Krauss, K.-E. Jaeger, Z. Cao, W. Gärtner, *Photochem. Photobiol. Sci.* **2007**, *6*, 41–49.
[31] G. Bernhardt, R. Rudolph, R. Jaenicke, *Z. Naturforsch. C* **1981**, *36*, 772–777.
[32] K. Huang, T. Merkle, C. F. Beck, *Physiol. Plant.* **2002**, *115*, 613–622.
[33] R. Hermann, R. Rudolph, R. Jaenicke, *Nature* **1979**, *277*, 243–245.
[34] U. K. Laemmli, *Nature* **1970**, *227*, 680–685.
[35] P. Reymond, T. W. Short, W. R. Briggs, K. L. Kenneth, *Proc. Natl. Acad. Sci. USA* **1992**, *89*, 4718–4721.
[36] J. M. Palmer, T. W. Short, S. Gallagher, W. R. Briggs, *Plant Physiol.* **1993**, *102*, 1211–1218.
[37] W. H. Press, B. P. Flannery, S. A. Teukolsky, W. T. Vetterling, *Numerical Recipes in C*, Cambridge University Press, Cambridge **1988**, p. 447.
[38] A. K. Livesey, P. Licinio, M. Delaye, *J. Chem. Phys.* **1986**, *84*, 5102–5107.
[39] A. Pedretti, L. Villa, G. Vistoli, *J. Mol. Graphics* **2002**, *21*, 47–49.
[40] W. L. DeLano, The PyMOL Molecular Graphics System **2002**, DeLano Scientific, Palo Alto, CA, USA; http://www.pymol.org

Received: November 11, 2007
Revised: March 12, 2008
Published online on July 4, 2008

